Asymptomatic parental mosaicism for osteogenesis imperfecta associated with a new splice site mutation in COL1A2.

Frederiksen, Anja Lisbeth; Dunø, Morten; Johnsen, Iben Birgit Gade; Frost, Morten; Krøigård, Anne Bruun

Published in:
Clinical Case Reports

DOI:
10.1002/ccr3.658

Publication date:
2016

Document version
Final published version

Document license
CC BY-NC

Citation for pulished version (APA):
Frederiksen, A. L., Dunø, M., Johnsen, I. B. G., Frost, M., & Krøigård, A. B. (2016). Asymptomatic parental mosaicism for osteogenesis imperfecta associated with a new splice site mutation in COL1A2. *Clinical Case Reports*, *4*(10), 972-978. https://doi.org/10.1002/ccr3.658

Clinical Case Reports

Open Access

CASE REPORT

Asymptomatic parental mosaicism for osteogenesis imperfecta associated with a new splice site mutation in *COL1A2*

Anja Lisbeth Frederiksen[1,5], Morten Duno[2], Iben B. G. Johnsen[3], Morten Frost Nielsen[4] & Anne Bruun Krøigård[1,3]

[1]Department of Clinical Genetics, Odense University Hospital, Odense, Denmark
[2]Department of Clinical Genetics, University Hospital Copenhagen, Copenhagen, Denmark
[3]Department of Clinical Pathology, Odense University Hospital, Odense, Denmark
[4]Department of Endocrinology, Odense University Hospital, Odense, Denmark
[5]Department of Clinical Research, Faculty of Health, University of Southern Denmark

Correspondence
Anne Bruun Krøigård, Department of Clinical Genetics, Odense University Hospital, Sdr. Boulevard 29, DK-5000 Odense, Denmark.
Tel: +45 29783054; Fax: +45 65414875;
E-mail: anne.kroeigaard@rsyd.dk

Funding Information
No sources of funding were declared for this study.

Received: 18 January 2016; Revised: 26 May 2016; Accepted: 11 July 2016

Clinical Case Reports **2016; 4(10): 972–978**

doi: 10.1002/ccr3.658

Key Clinical Message

Recurrent lethal perinatal osteogenesis imperfecta may result from asymptomatic parental mosaicism. A previously unreported mutation in *COL1A2* leads to recurrent cases of fetal osteogenesis imperfecta Sillence type IIA, which emphasizes the importance of clinical and genetic evaluation of mosaicism in asymptomatic parents as verified mosaicism highly increases recurrence risk.

Keywords

COL1A2, mosaicism, osteogenesis imperfecta type IIA, splice site mutation.

Introduction

Osteogenesis imperfecta (OI), or brittle bone disease, is a phenotypically and molecularly heterogeneous group of genetic connective tissue disorders that occurs in one in 15,000–20,000 births [1]. The phenotypic appearance ranges from minimal bone fragility, decreased bone mass, blue sclerae, hyperlaxity of skin and ligaments, dentinogenesis imperfecta, and hearing loss to severe bone malformation and perinatal death caused by multiple fractures [2]. Based on clinical characteristics, Sillence et al. classified OI patients into four groups [3]. Laboratory testing for OI may include either biochemical testing of collagen or, increasingly, next-generation sequencing (NGS) of genes associated with OI. At present, 17 genes associated with OI and closely related disorders have been identified [4]. In 90% of cases, heterozygous mutations in the *COL1A1* or *COL1A2* genes, encoding the alpha 1 and alpha 2 chains of collagen type I, respectively, are responsible for the phenotype [5]. Collagen type I is the most abundant protein of skin, bone, and tendon extracellular matrices. The nondeforming OI (Sillence type I) is related to quantitative deficiency of structurally normal collagen, whereas lethal OI (type II), progressively deforming (type III), and common variable (type IV) mainly result from mutations that alter the collagen structure [1]. *COL1A1*- and *COL1A2*-related OI are inherited in an autosomal dominant manner. For OI types II-IV, the intertwining of mutated and normal collagen type I chains results in production of abnormal collagen type I protein, which is rapidly degraded, explaining the dominant negative effect of the mutations [4]. A number of genes, including but not restricted to cartilage-associated protein (CRTAP) and prolyl-3-hydroxylase-1 (P3H1, encoded by the *LEPRE1* gene), have recently been identified to be involved in autosomal recessive OI. Thus, advances in molecular diagnostics have identified new OI subtypes [6].

Severe and perinatal lethal OI can be classified as Sillence type II, (OMIM #166210). The condition may be detected by an abnormal ultrasound scan around 20 weeks of gestation. The fetus presents with growth retardation, shortening, and bowing of long bones which are severely under-modeled and crumbled [4]. Multiple fractures of the ribs leads to a beaded appearance of the ribs (Sillence type IIA) or ribs can be thin (Sillence type IIB) [4]. The postnatal presentation includes multiple fractures, small thorax, decreased ossification of the skull, and respiratory distress [7]. More than 60% of affected infants die within the first day, and survival beyond 1 year is extremely rare [2].

Children with autosomal dominant inherited osteogenesis imperfecta may be born from unaffected parents due to parental mosaicism [8–12]. We present a family in which a case of lethal perinatal OI, Sillence type IIA, in a fetus lead to the discovery of parental mosaicism for a previously unreported synonymous mutation, c. 1863G>A, p.Lys621Lys in the *COL1A2* gene presumed to affect correct mRNA splicing. The fetus in the consecutive pregnancy was also affected. The study emphasizes the importance of clinical and genetic assessment for parental mosaicism as this strongly influences recurrence risk.

Methods

Genetic analysis

DNA was isolated from the different specimens by standard methods. The entire coding and exon flanking sequences of *COL1A1* (NM_000088.3) and *COL1A2* (NM_000089.3) were amplified by means of a custom designed AmpliSeq capture assay, using the Ion Ampliseq Lib 2.0 assay (Thermo Fisher Scientific, Waltham, USA). Sequence-ready libraries were generated on the IonChef and subsequently sequenced on the IonPGM (Thermo Fisher Scientific, Waltham, USA) using HiQ chemistry on a 318v2 chip (Ion PGM™ IC 200 Kit, Waltham, USA). All procedures were carried out according to the manufacturer's description (Thermo Fisher Scientific). Samples were sequenced to a minimum mean depth of 500x. Areas with low coverage (<30x) were Sanger sequenced. Variants were filtered against the UCSC common SNP panel (SNP142), and subsequent variants were manually curated and confirmed by standard Sanger sequencing (primers and PCR conditions are available upon specific request).

The level of mosaicism is expressed as allele frequencies determined directly from the next-generation sequencing data. The sequencing depth of the c.1863 position was 1043, 876, and 883 in DNA isolated from blood, buccal, and saliva cells, respectively.

Bone parameters

Areal bone mineral density (aBMD) was measured at the lumbar spine, hip region, wrist, and whole body using dual energy X-ray absorptiometry (DXA) (Hologic Discovery, Waltham, MA). T-scores were calculated using the reference range provided by the manufacturer and the Third National Health and Nutrition Examination Survey reference [13].

A high-resolution peripheral quantitative computed tomography (HR-pQCT) system (XtremeCT, Scanco Medical AG, Brüttisellen, Switzerland) was used to assess bone geometry, volumetric bone mineral density (vBMD), and microarchitecture of radius and tibia in left and right extremities. The default protocol for *in vivo* imaging was applied providing a 9.02 mm axial 3D bone representation at each site. The offset from the endplate to the measurement region was 9.5 and 22.5 mm at the distal radius and tibia, respectively, with the scan region extending proximally. Each scan consisted of 110 parallel CT slices resulting in an 82 μm isotropic voxel size. Attenuation data were converted to equivalent hydroxyapatite (HA) densities, and measures of total, cortical, and trabecular microarchitecture were computed using the standard manufacturer's software [14]. A phantom was scanned daily for quality control (QRM, Möhrendorf, Germany).

Standardized algorithms were used to separate the bone into cortical and trabecular compartments, and calculate trabecular bone volume per tissue volume (BV/TV), trabecular number (Tb.N), trabecular thickness (Tb.Th), and trabecular spacing (Tb.Sp) as previously described [15].

Biochemical evaluation

Biochemical evaluation was performed with automated techniques in an accredited laboratory including use of liquid chromatography–mass spectrometry (LC-MS) technique and Architect c16000 (Abbott Diagnostics).

Results

Clinical report

A healthy, nonconsanguineous couple, who previously gave birth to a healthy daughter, family pedigree shown in Figure 1, was referred to genetic counseling after termination of a pregnancy at 19 weeks of gestation due to a clearly abnormal ultrasound scan showing growth restriction and a small thorax leading to suspicion of thanatophoric dysplasia. The aborted fetus was initially assessed for thanatophoric dysplasia by direct sequencing of the coding regions of the *FGFR3* gene, but no mutations were detected. Pathological examination of the fetus

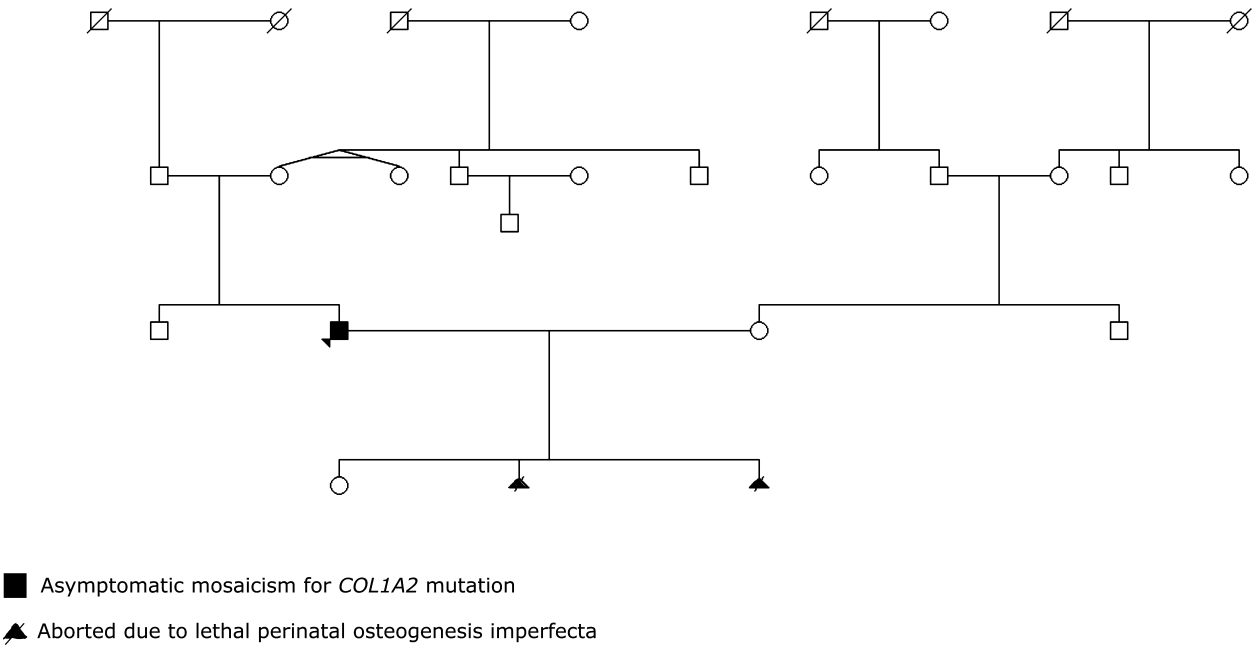

Figure 1. Family pedigree.

showed growth retardation, an abnormally shaped head, shortening and bowing of the long bones, fractures of the femora, decreased ossification of the skull, multiple rib fractures of different ages, and very soft bone tissue in accordance with the clinical phenotype OI. Radiograph of the aborted fetus is shown in Figure 2. Mutational analysis on fetal DNA revealed that the aborted fetus was heterozygous for a synonymous variant c. 1863G>A, p.Lys621Lys in the *COL1A2* gene, Sanger sequencing shown in Figure 3. The variant has, to our knowledge, not been previously described and is accordingly not reported in the Human Gene Mutation Database [16], in the *COL1A2* locus database (https://oi.gene.le.ac.uk/home.php?select_db=COL1A2), or in the Exome Aggregation Consortium (ExAC) database. The variant does not result in an amino acid change, but affects the last nucleotide of exon 31, which according to in silico prediction tools destroys the 5′ splice site.

The mutation was not detected in full blood-derived DNA from the mother. In a full blood-derived DNA sample from the father, the variant was detected with an allele frequency of 33%, which lead to mutational analysis of his parents. The variant was, as expected, not present in full blood-derived DNA from the parents. Hence, the mutation is likely a result of a postzygotic de novo event in the father. Based on the clinical findings, in silico predictions, and the fact that it is a *de novo* event, the variant was categorized as pathogenic and causal for the fetal phenotype. The mosaic nature of the mutation was confirmed as DNA analysis on buccal cells and cells from saliva revealed mutant allele frequencies of 19% and 33%, respectively. The mother became pregnant again, and a chorion villus biopsy was taken at 12 weeks of gestation.

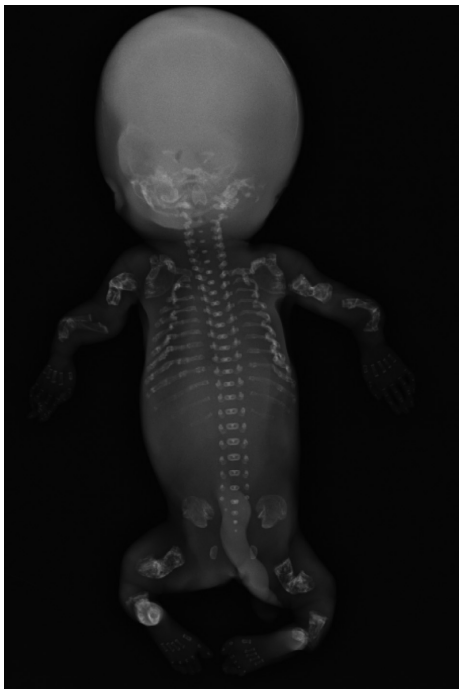

Figure 2. Radiograph of the first aborted fetus at 19 weeks of gestation showing shortening and bowing of the long bones, fractures of the femora, decreased ossification of the skull, and multiple rib fractures of different ages in accordance with the clinical phenotype OI.

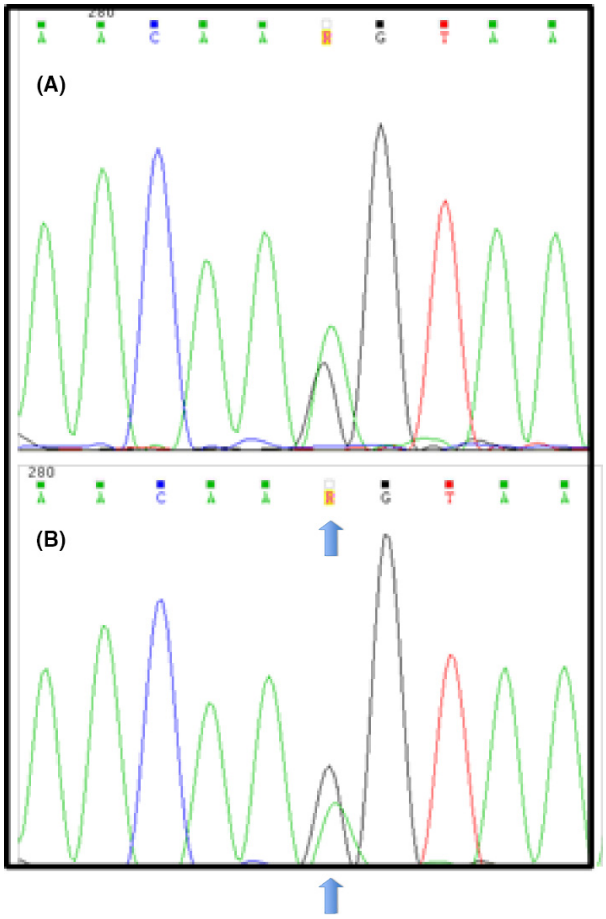

Figure 3. Sanger sequence of c. 1863G>A in *COL1A2*. A. Fetal sequence, B. Paternal sequence depicting the mosaicism nature. Unfortunately, the quality of this image cannot be improved as the original file is of the same quality.

Mutation analysis of chorion villus DNA showed that this fetus was heterozygous for the same mutation in the *COL1A2* gene and the pregnancy was subsequently terminated. No detailed pathological examination was performed, but the fetus at 15 weeks of gestation, was small for gestational age, and presented postpartum with clear clinical signs of OI in the form of narrow chest and short and bowed extremities. In both OI pregnancies, ultrasound scans at 12 weeks of gestation were reported as normal.

Phenotype of case with OI mosaicism

The father, age 34, had lived an active, healthy life. Clinical examination showed normal height, normal sclerae, normal dental status, and normal configuration of extremities. Neither chest wall deformities nor joint hypermobility or hyperlaxity of the skin was observed. The only abnormal finding was unilateral difference in the size of the extremities as the left arm and leg were of smaller size compared to extremities on the right side, shown in Figure 4. The left arm was 0.5 cm shorter than the right arm, and the left hand was 0.5 cm shorter than the right hand. The difference in leg length was 1.5 cm. He had a history of fractures of the clavicular, scaphoid, and metatarsal bones, which were related to high-energy trauma.

Standard DXA assessment of the lumbar spine, hip region, wrist, and whole body (Table 1) showed normal bone mineral density as compared to standards defined by World Health Organization [17] and no significant differences between left- and right-sided extremities. Standard HR-pQCT of the radius and tibia (Table 2) revealed normal geometry, volumetric bone mineral density, and microarchitecture, and most parameters do not differ significantly from age- and gender-matched normal material [18]. Again, no significant differences between the two sides were found. Biochemical evaluation was normal with hemoglobin 8.9 mmol/L (8.3–10.5 mmol/L), 25-OH vitamin D 79 nmol/L (50–160 nmol/L), thyroid-stimulating hormone 1.1 10^{-3} IU/L (0.5–4.3 10^{-3} IU/L), follicle-stimulating hormone 6.1 IU/L (1.1–7.9 IU/L), luteinizing hormone 6.8 IU/L (1.5–11 IU/L), sex hormone-binding globulin 63.2 nmol/L (13–55 nmol/L), and testosterone 23.5 nmol/L (8.40–30.0 nmol/L).

Discussion

We present a novel synonymous mutation in *COL1A2* possibly affecting correct mRNA splicing associated with OI Sillence type IIA and parental mosaicism for the mutation, detected by NGS. We report normal bone morphology in the mosaic father, evaluated by DXA scan and HR-pQCT. The asymmetry in body composition with slightly reduced size of left-sided extremities in the father is unlikely to result from the OI mosaicism as this phenomenon may be due to a number of factors [19] and is not a distinctive feature of OI.

The incidence of mosaicism is most likely highly underestimated [20]. Low-grade mosaicism is very difficult to detect by the previous traditional Sanger sequencing. Although NGS provides a new diagnostic tool for identifying genetic mosaicism, it can easily be missed as biased allele calls are filtered out in the bioinformatic workflow. Revisions of current diagnostic laboratory protocols are needed in order to increase the detection rate of mosaic cases [21]. An unknown proportion of mutations categorized as *de novo* may in fact result from unrecognized parental mosaicism [20]. Asymptomatic parental somatic mosaicism has recently been identified by NGS and reported for a number of rare diseases such as Alport syndrome, tuberous sclerosis, and Dravet syndrome [22–25].

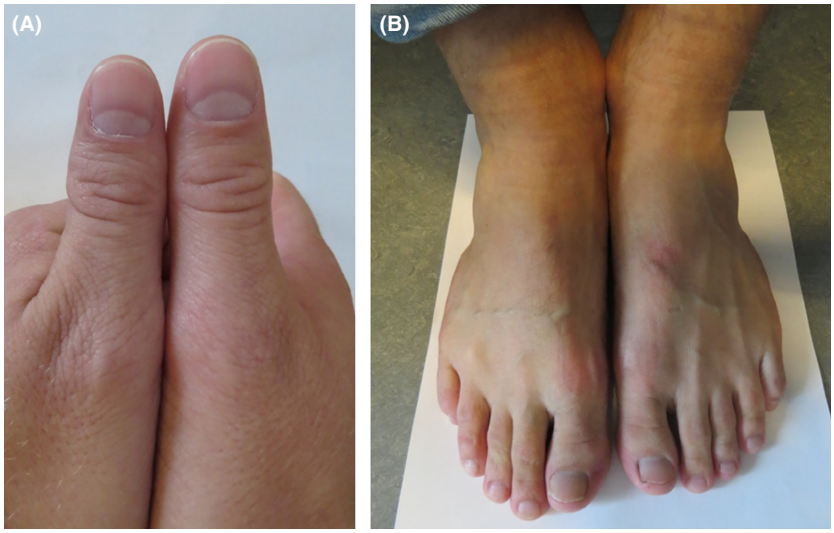

Figure 4. Reduced size of left-sided extremities of the male patient with OI mosaicism. A. The left thumb is smaller than the right thumb. B. The left foot is smaller than the right foot.

Table 1. T-scores and Z-scores evaluated by dual energy X-ray absorptiometry (DXA) scan.

	Left side (SD)	Right side (SD)
Lumbar spine, total BMD, T-score	−0.7	−0.7
Lumbar spine, total BMD, Z-score	−0.7	−0.7
Hip, total BMD, T-score	0.5	0.1
Hip, total BMD, Z-score	0.6	0.2
Wrist, total BMD, T-score	−2.0	−1.1
Wrist, total BMD, Z-score	−1.9	−1.0
Whole body scan, total BMD, T-score	−0.4	−0.4
Whole body scan, total BMD, Z-score	−0.5	−0.5

The T-score, in units of standard deviation (SD), indicates the standard deviation from the normal values of a healthy 30 years old of the same sex. The Z-score, in units of standard deviation (SD), indicates the standard deviation from the normal values of an age-matched person of the same sex. According to definitions defined by the World Health Organization a T-score of −1.0 and above indicates normal bone density, T-score between −1.0 and −2.5 indicates osteopenia, and a T-score −2.5 and lower indicates osteoporosis in men aged more than 50 years [17]. BMD, bone mineral density.

Table 2. Geometry, volumetric bone mineral density, and microarchitecture evaluated by high-resolution peripheral quantitative computed tomography (HR-pQCT).

	Left side	Right side
Radius		
Cortical bone area (mm^2) (75 mm^2)	75.9	77.6
Cortical thickness (mm) (1.02 mm)	1.07	1.00
Cortical bone density (mg/cm^3) (873 mg/cm^3)	926.1	904.8
Trabecular bone density (mg/cm^3) (199 mg/cm^3)	219.5	212.1
Trabecular BV/TV (%) (16.5%)	18.3	17.7
Trabecular bone area (mm^2) (278 mm^2)	195.3	256.2
Trabecular number (per mm) (2.06/mm)	1.78	2.12
Trabecular thickness (mm) (0.080 mm)	0.103	0.083
Trabecular spacing (mm) (0.406 mm)	0.460	0.389
Tibia		
Cortical bone area (mm^2) (160 mm^2)	199.7	192.7
Cortical thickness (mm) (1.31 mm)	1.99	1.83
Cortical bone density (mg/cm^3) (876 mg/cm^3)	928.8	909.2
Trabecular bone density (mg/cm^3) (218 mg/cm^3)	262.5	269.9
Trabecular BV/TV (%) (18.1%)	21.9	22.5
Trabecular bone area (mm^2) (737 mm^2)	439.1	504.3
Trabecular number (per mm) (2.20/mm)	2.06	2.10
Trabecular thickness (mm) (0.083 mm)	0.106	0.107
Trabecular spacing (mm) (0.362 mm)	0.379	0.369

Normal values [18] in parentheses. BV/TV, bone volume per tissue volume.

Genomic mosaicism results from postzygotic events occurring predominantly in early embryogenesis but can arise throughout life and results in genetically distinct cell lines within one individual. During cell division, errors in chromosome segregation or DNA replication occur and may lead to aneuploidy, copy number variations, genome rearrangements, repeat expansions, microsatellite instabilities, or single-nucleotide variations [26]. Selection against the mutation can occur and the clinical manifestations can range from none or minimal to a segmental or severe generalized effect [27]. The selection pressure is tissue-dependent as a mutation can be strongly selected against in tissues in which the gene product is essential to cell function, whereas the same mutation is tolerated in other somatic cells [27]. Individuals with mosaicism for

autosomal dominant OI are often asymptomatic or present with subtle clinical manifestations and are only identified when having a second child with the condition. A negative selection process in tissues where collagen is of great importance may be an explanation for the lack of a recognized phenotype [12]. This highlights the need for sensitive methods like NGS and suggests that more than one tissue should be examined.

Osteoporosis develops in the majority of patients with complete OI, and analyses of bone histomorphometry have revealed increased bone formation and increased bone resorption with a net effect of a small progressive bone loss [4]. Altered bone microstructure and bone geometry, evaluated by HR-pQCT, has been reported in patients with OI types I, III, and IV [28, 29]. However, in two mosaic carriers, normal skeletal growth, bone density, and bone histology were found in spite of 40–75% burden of osteoblasts heterozygous for a *COL1A1* mutation [30], which is concordant with our findings.

In conclusion, we report a family affected by two cases of fetal OI, Sillence type IIA, as a result of parental mosaicism for a previously unreported synonymous mutation in the *COL1A2* gene. The mosaic father was clinically unaffected, and evaluation of bone morphology by DXA scan and HR-pQCT revealed normal bone structure. As collagen most likely has no functional importance in spermatocytes, no negative selection pressure exists and the risk of OI pregnancies is related to the proportion of germ cells with the mutation. A surprisingly large proportion of assumed *de novo* mutations may in fact be related to low-grade parental mosaicism.

Consent

Written informed consent was obtained from the patients.

Acknowledgment

The authors thank the family for participating in the study.

Conflict of Interest

All authors state that they have no conflict of interest.

References

1. Forlino, A., and J. C. Marini. 2015. Osteogenesis imperfecta. Lancet 387:1657–1671.
2. Steiner, R. D., J., Adsit, and D. Basel. 1993. COL1A1/2-Related Osteogenesis Imperfecta. I: Pagon RA, Adam MP, Ardinger HH, Wallace SE, Amemiya A, Bean LJ, m.fl., redaktører. GeneReviews(®) [Internet]. University of Washington, Seattle, Seattle, WA. [henvist 16. November 2015]. Hentet fra: http://www.ncbi.nlm.nih.gov/books/NBK1295/
3. Sillence, D. O., A. Senn, and D. M. Danks. 1979. Genetic heterogeneity in osteogenesis imperfecta. J. Med. Genet. 16:101–116.
4. Van Dijk, F. S., and D. O. Sillence. 2014. Osteogenesis imperfecta: clinical diagnosis, nomenclature and severity assessment. Am. J. Med. Genet. A 164A:1470–1481.
5. van Dijk, F. S., J. M. Cobben, A. Kariminejad, A. Maugeri, P. G. J. Nikkels, R. R. van Rijn, et al. 2011. Osteogenesis imperfecta: a review with clinical examples. Mol. Syndromol. 2:1–20.
6. Valadares, E. R., T. B. Carneiro, P. M. Santos, A. C. Oliveira, and B. Zabel. 2014. What is new in genetics and osteogenesis imperfecta classification? J. Pediatr. (Rio. J.) 90:536–541.
7. Ayadi, I. D., E. B. Hamida, R. B. Rebeh, S. Chaouachi, and Z. Marrakchi. 2015. Perinatal lethal type II osteogenesis imperfecta: a case report. Pan Afr. Med. J. 21:11.
8. Cohn, D. H., B. J. Starman, B. Blumberg, and P. H. Byers. 1990. Recurrence of lethal osteogenesis imperfecta due to parental mosaicism for a dominant mutation in a human type I collagen gene (COL1A1). Am. J. Hum. Genet. 46:591–601.
9. Chen, C.-P., S.-P. Lin, Y.-N. Su, S.-R. Chern, J.-W. Su, and W. Wang. 2013. Prenatal diagnosis of recurrent autosomal dominant osteogenesis imperfecta associated with unaffected parents and paternal gonadal mosaicism. Taiwan J. Obstet. Gynecol. 52:106–109.
10. Raghunath, M., K. Mackay, R. Dalgleish, and B. Steinmann. 1995. Genetic counselling on brittle grounds: recurring osteogenesis imperfecta due to parental mosaicism for a dominant mutation. Eur. J. Pediatr. 154:123–129.
11. Lund, A. M., M. Schwartz, and F. Skovby. 1996. Genetic counselling and prenatal diagnosis of osteogenesis imperfecta caused by paternal mosaicism. Prenat. Diagn. 16:1032–1038.
12. Namikawa, C., K. Suzumori, Y. Fukushima, M. Sasaki, and A. Hata. 1995. Recurrence of osteogenesis imperfecta because of paternal mosaicism: Gly862–>Ser substitution in a type I collagen gene (COL1A1). Hum. Genet. 95: 666–670.
13. Hanson, J. 1997. Standardization of femur BMD. J. Bone Miner. Res. 12:1316–1317.
14. Boutroy, S., M. L. Bouxsein, F. Munoz, and P. D. Delmas. 2005. In vivo assessment of trabecular bone microarchitecture by high-resolution peripheral quantitative computed tomography. J. Clin. Endocrinol. Metab. 90:6508–6515.

15. Frederiksen, A. L., S. Hansen, K. Brixen, and M. Frost. 2014. Increased cortical area and thickness in the distal radius in subjects with SHOX-gene mutation. Bone 69:23–29.
16. Stenson, P. D., M. Mort, E. V. Ball, K. Shaw, A. Phillips, and D. N. Cooper. 2014. The Human Gene Mutation Database: building a comprehensive mutation repository for clinical and molecular genetics, diagnostic testing and personalized genomic medicine. Hum. Genet. 133:1–9.
17. World Health Organ. 2003. Prevention and management of osteoporosis. World Health Organ. Tech. Rep. Ser. 921:1–164, back cover.
18. Hansen, S., V. Shanbhogue, L. Folkestad, M. M. F. Nielsen, and K. Brixen. 2014. Bone microarchitecture and estimated strength in 499 adult Danish women and men: a cross-sectional, population-based high-resolution peripheral quantitative computed tomographic study on peak bone structure. Calcif. Tissue Int. 94:269–281.
19. Auerbach, B. M., and C. B. Ruff. 2006. Limb bone bilateral asymmetry: variability and commonality among modern humans. J. Hum. Evol. 50:203–218.
20. Campbell, I. M., B. Yuan, C. Robberecht, R. Pfundt, P. Szafranski, M. E. McEntagart, et al. 2014. Parental somatic mosaicism is underrecognized and influences recurrence risk of genomic disorders. Am. J. Hum. Genet. 95:173–182.
21. Gajecka, M. 2016. Unrevealed mosaicism in the next-generation sequencing era. Mol. Genet. Genomics 291: 513–530.
22. Beicht, S., G. Strobl-Wildemann, S. Rath, O. Wachter, M. Alberer, E. Kaminsky, et al. 2013. Next generation sequencing as a useful tool in the diagnostics of mosaicism in Alport syndrome. Gene 526:474–477.
23. Acuna-Hidalgo, R., T. Bo, M. P. Kwint, M. van de Vorst, M. Pinelli, J. A. Veltman, et al. 2015. Post-zygotic point mutations are an underrecognized source of de novo genomic variation. Am. J. Hum. Genet. 97:67–74.
24. Qin, W., P. Kozlowski, B. E. Taillon, P. Bouffard, A. J. Holmes, P. Janne, et al. 2010. Ultra deep sequencing detects a low rate of mosaic mutations in tuberous sclerosis complex. Hum. Genet. 127:573–582.
25. Huang, A. Y., X. Xu, A. Y. Ye, Q. Wu, L. Yan, B. Zhao, et al. 2014. Postzygotic single-nucleotide mosaicisms in whole-genome sequences of clinically unremarkable individuals. Cell Res. 24:1311–1327.
26. Lupski, J. R. 2013. Genetics. Genome mosaicism–one human, multiple genomes. Science 341:358–359.
27. Youssoufian, H., and R. E. Pyeritz. 2002. Mechanisms and consequences of somatic mosaicism in humans. Nat. Rev. Genet. 3:748–758.
28. Folkestad, L., J. D. Hald, S. Hansen, J. Gram, B. Langdahl, B. Abrahamsen, et al. 2012. Bone geometry, density, and microarchitecture in the distal radius and tibia in adults with osteogenesis imperfecta type I assessed by high-resolution pQCT. J. Bone Miner. Res. 27:1405–1412.
29. Kocijan, R., C. Muschitz, J. Haschka, D. Hans, A. Nia, A. Geroldinger, et al. 2015. Bone structure assessed by HR-pQCT, TBS and DXL in adult patients with different types of osteogenesis imperfecta. Osteoporos. Int. 26: 2431–2440.
30. Cabral, W. A., and J. C. Marini. 2004. High proportion of mutant osteoblasts is compatible with normal skeletal function in mosaic carriers of osteogenesis imperfecta. Am. J. Hum. Genet. 74:752–760.

Supporting Information

Additional Supporting Information may be found online in the supporting information tab for this article:

Figure S1. High-resolution peripheral quantitative computed tomography (HR-pQCT) scan images. A. left radius. B. Right radius.

Figure S2. High-resolution peripheral quantitative computed tomography (HR-pQCT) scan images. A. left tibia. B. Right tibia.